

Polymorphs and Solvates of Nicardipine Hydrochloride. Selective Stabilization of Different Diastereomeric Racemates

Evelyn Moreno-Calvo,^{†,‡} María Muntó,^{†,‡} Klaus Wurst,[§] Nora Ventosa,^{*,†,‡} Norberto Masciocchi,^{*,||} and Jaume Veciana^{†,‡}

[†]Institut de Ciència de Materials de Barcelona (CSIC), Campus Universitari de Bellaterra, 08193 Cerdanyola del Vallès, Spain

[‡]CIBER de Bioingeniería, Biomateriales y Nanomedicina (CIBER-BBN), Barcelona, Spain

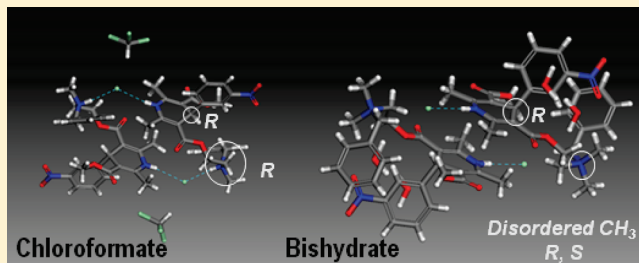
[§]Institute of General, Inorganic and Theoretical Chemistry, University of Innsbruck, Innrain 52a, A-6020 Innsbruck, Austria

^{||}Dipartimento di Scienze Chimiche e Ambientali, Università dell'Insubria, via Valleggio 11, 22100 Como, Italy

 Supporting Information

ABSTRACT: Molecular understanding of the drug nicardipine hydrochloride (NHc) is provided within this study. For this reason, the polymorphism and crystal structures, including stereochemistry, of the known and the new discovered polymorphs of NHc are discussed. Three new crystalline forms of the nicardipine hydrochloride drug have been isolated: (i) a bishydrated phase, (ii) a chloroform solvate and (iii) a toluene hemisolvate. The crystal structures of these new solvated phases and those of the previously known α and β polymorphs have been determined from conventional single-crystal X-ray diffraction analysis (α phase and chloroform solvate) or from high quality powder X-ray diffraction data using direct-space methods (β phase, bishydrate and toluene hemisolvate). The analysis of the crystal structures revealed that nicardipine hydrochloride crystallizes, in all studied phases, as a racemate with the organic moiety adopting different diastereoisomeric configurations (addressed by the presence of two stereocenters, the C1 and N3 atoms) depending on the actual solvent or polymorph. The chirality of the protonated nicardipine molecules is driven, in the solids, by the strong electrostatic interactions between chloride ions and the protonated nitrogen atoms, which result, in the α phase and in the chloroform solvate, in centrosymmetric dimers built by R,R and S,S molecules. At variance, the β polymorph contains R,S and S,R molecules, still arranged in dimers, but possessing a markedly different molecular shape. Interestingly, in the bishydrated and toluene hemisolvate phases, a slightly disordered crystal structure about the positively charged ammonium group is formed, and both diastereoisomeric couples are present (although with different site occupation factors).

KEYWORDS: nicardipine hydrochloride, polymorphism, racemates, crystals of diastereoisomeric molecules, structure determination from powder diffraction data



INTRODUCTION

Nicardipine hydrochloride (Scheme 1), hereafter referred to as NHc, is a polysubstituted 1,4-dihydropyridine-based drug with extended therapeutic properties. It is known to act as a calcium antagonist widely employed in the treatment of some cardiovascular and cerebrovascular disorders and also for the treatment of esophageal cancer in animals.^{1–6} Presently, NHc is commercially available in injectable solutions as well as pellets and powders, in which it is found in the β form.⁷ However, the use of NHc is actually limited by its poor solubility in body fluids and its almost complete (up to 80%) degradation in the liver.^{1–4} Since polymorphism—the ability of a compound to give at least two different arrangement of the molecules in the solid state—affects the physicochemical properties of a given compound, its study is crucial in the development of drugs and drug delivery systems.^{8,9} Thus, one strategy of overcoming the limitations of the actual formulation of

NHc drug could be the obtaining of new polymorphs with lower packing coherence and stability.

Nicardipine hydrochloride was first isolated by Iwatani et al. (1979)¹⁰ and later characterized by Yan and Guiunchedi (1990).¹¹ From the structural point of view, NHc is a polysubstituted 1,4-dihydropyridine with two chiral centers, one located at the asymmetric carbon of the dihydropyridine ring (1) and the second located at the protonated tertiary amine (2). The presence in the molecule of two chemically uncorrelated stereocenters generates diastereoisomeric molecules (R,R , R,S and their enantiomers: all likely copresent, although in different amounts, in solution), which could be isolated by thermodynamically or kinetically controlled

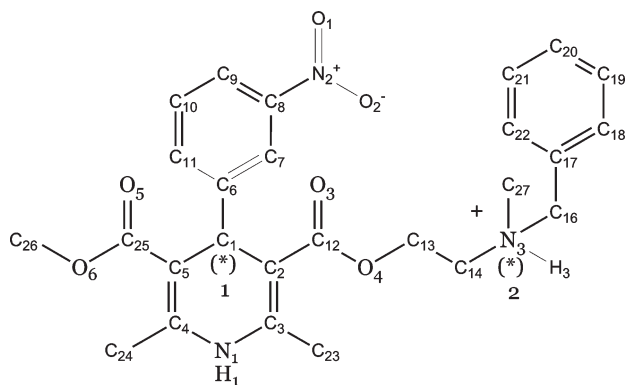
Received: July 30, 2010

Accepted: December 17, 2010

Revised: December 10, 2010

Published: December 17, 2010

Scheme 1. Molecular Formula of the N-Protonated Nicardipine Molecule (the Nicardipinium Ion) with Atomic Numbering Scheme^a



^a The two stereocenters (C₁ and N₃) have been marked with an asterisk.

crystallization processes.¹² As such, precipitation of one phase over the other, i.e. selective separation of one diastereoisomeric couple, is *per se* a purification process, driven, in this case, by subtle, but reproducible, changes (temperature, stirring, solvent polarity, etc.). The preferential (low temperature) formation of racemates over conglomerates of enantiomeric crystals for Pasteur's tartaric acid is a paradigmatic example of this kind of selectivity.¹³ In the present case, chiral phases have not been detected, but the separation of diastereoisomers (rather than enantiomeric ones) follows the same logical path.

The molecular structure of NHc reveals that this molecule possesses several internal rotational degrees of freedom. It is therefore of no surprise that NHc exhibits both a glassy phase and a variety of polymorphs and solvated forms.^{8,9} However, in the scientific literature only one amorphous and two crystalline forms of NHc (α and β , melting at 453 and 440 K, respectively) of unknown crystal structures were reported.¹¹ Coherently with its lower melting point and higher solubility, the form β was claimed to be metastable with respect to form α . Rationalization of the crystal structures of the different polymorphs and solvates of NHc and their polymorphic transformation on the basis of the intermolecular interactions constitute the main subject of this paper.

The serendipitous discovery of a new crystalline phase (CHCl₃-solvated NHc) when this calcium entry blocker was crystallized from carbon dioxide expanded chloroform using the Gas Antisolvent^{14–18} (GAS) and the Depressurization of an Expanded Liquid Organic Solution^{14–18} (DELOS) methodologies encouraged us to study in more depth the polymorphism of this drug.¹² Moreover, the lack of structural information and newly discovered (pseudo)polymorphism of the NHc drug motivated us to investigate the crystal structures of the so-called α and β polymorphs and the newly isolated NHc solvated, aiming at a deeper understanding of the structure-driven macroscopic effects, among which are stability and solubility.

This paper focuses on two different aspects: on one hand, new crystalline phases of NHc have been prepared from standard crystallization methodologies and fully characterized, their crystal structures have been determined and their solid state stereochemistry has been rationalized. On the other hand, the extensive use of X-ray powder diffraction (XRPD) methods as a structural tool in modern chemists' hands witnesses the power of this unconventional technique also when using well-conditioned laboratory equipment

on materials not affording single crystals of suitable size and quality.¹⁹

MATERIALS AND METHODS

Materials. Raw nicardipine hydrochloride (purity 98%, β phase) was purchased from Roig Pharma (Barcelona, Spain). All organic solvents used were purchased from Romil Chemicals (Cambridge, U.K.) and used without further purification. Carbon dioxide (purity >99%) was kindly supplied by S.E. Carburos Metálicos (Barcelona, Spain).

Crystallization Experiments. Single crystals of the α phase, suitable for conventional X-ray diffraction structural analysis, were prepared by evaporation of a nitromethane saturated solution (20 mL) during two weeks at room temperature and in the absence of light. Single crystals of the chloroform solvate were prepared by slow diffusion of diethyl ether over a NHc chloroform solution at 255 K. A polycrystalline sample of the β phase, suitable for structure determination from XRPD data, was obtained by cooling an unstirred saturated solution (5 mL) of NHc in methanol from 308 to 253 K. A polycrystalline sample of the hydrated phase of NHc was prepared by exchanging the chloroform present in the CHCl₃ solvate prepared as reported previously with water by suspending the chloroform phase in humid ethyl ether (500 μ L to 1 mL) at 281 K during one week. A polycrystalline sample of the toluene hemisolvate of NHc was prepared by dissolving NHc (1 g) in a toluene/methanol (ratio 3:1) solvent mixture (40 mL), at 313 K; next, methanol was eliminated by moderate heating at 333 K until the formation of a precipitated was observed; this suspension was then cooled down to 273–278 K under vigorous stirring, the toluene hemisolvate being quantitatively recovered after some hours.

Supercritical Drying. The chloroform solvate (100 mg) of NHc was dried during 8 h with supercritical CO₂ at $P = 13$ MPa and $T = 313$ K.

Thermal Analysis. Differential scanning calorimetric measurements were performed with the aid of a Perkin-Elmer DSC-7 calorimeter. Samples (2.5–3.0 mg) were loaded in aluminum pans and heated at a constant rate of 5 K min⁻¹, under argon (30 mL/min), from 313 K beyond melting. The instrument was calibrated using indium and zinc as external standards. The systematic uncertainties of temperatures and heat flow calibration coefficients for the DSC were evaluated as ± 0.2 K and $\pm 2\%$, respectively.

Thermogravimetric analyses were recorded with a STA 449 F1 Jupiter (Netzsch) instrument. Samples of approximately 3 mg were loaded into 40 μ L aluminum pans and heated at 5 K min⁻¹ from 313 to 650 K, under a nitrogen purge (80 mL/min).

Crystal Structure Determination. *X-ray Powder Diffraction Analysis.* Strictly monophasic samples of NHc in its β phase and bishydrated and toluene hemisolvates were gently ground in an agate mortar, and then deposited in the hollow of a 0.2 mm deep aluminum sample holder, equipped with a quartz monocrystal zero background plate (supplied by *The Gem Dugout*, State College, PA). Diffraction data were collected in the 5–105° 2 θ range, sampling at 0.02°, on a θ : θ vertical scan Bruker AXS D8 Advance diffractometer, equipped with a linear LynxEye position sensitive detector, set at 300 mm from the sample; Ni-filtered Cu K α _{1,2} radiation, $\lambda = 1.5418$ Å. Standard peak search methods, followed by indexing by TOPAS-R,²⁰ allowed the determination of approximate cell parameters [M(20) values are reported in Table 1]. Systematic absences, where pertinent, and density considerations clearly indicated the corresponding space group, later confirmed by successful structure solution and refinement. Structure solution was initiated by employing a semirigid molecular

Table 1. Crystal Data and Refinement Details for the Nicardipine Hydrochloride, in Its α and β Phases and in the Three Solvated Phases

	α -NHc	β -NHc	bishydrated	toluene hemisolvate	chloroform solvate
empirical formula	$C_{26}H_{30}ClN_3O_6$	$C_{26}H_{30}ClN_3O_6$	$C_{26}H_{34}ClN_3O_8$	$C_{29.5}H_{34}ClN_3O_6$	$C_{27}H_{31}Cl_4N_3O_6$
fw, g mol ⁻¹	515.99	515.99	551.99	562.02	635.31
method	single-crystal	powder diffraction	powder diffraction	powder diffraction	single-crystal
λ , Å	Mo Ka, 0.71073	Cu Ka, 1.5418	Cu Ka, 1.5418	Cu Ka, 1.5418	Mo Ka, 0.71073
cryst syst	triclinic	triclinic	monoclinic	monoclinic	triclinic
SPGR, Z	$P\bar{1}$, 2	$P\bar{1}$, 2	$P2_1/c$, 4	$P2_1/c$, 4	$P\bar{1}$, 2
<i>a</i> , Å	8.2152(5)	10.4248(5)	11.3146(5)	11.5816(7)	11.3469(8)
<i>b</i> , Å	11.2043(6)	11.0795(6)	10.6872(7)	10.6978(9)	11.8907(8)
<i>c</i> , Å	14.574(9)	13.5127(6)	20.008(1)	23.799(2)	12.0830(4)
α , deg	102.999(4)	107.361(3)	90	90	86.389(4)
β , deg	90.879(4)	111.510(3)	99.128(4)	100.372(5)	67.744(4)
γ , deg	94.720(4)	100.980(3)	90	90	85.361(4)
<i>V</i> , Å ³	1301.87(13)	1304.5(1)	2866.3(3)	2900.4(4)	1502.95(16)
ρ_{calc} , g cm ⁻³	1.316	1.314	1.279	1.289	1.404
μ , cm ⁻¹	1.92	16.8	16.2	15.6	4.39
<i>T</i> , K	233(2)	298(2)	298(2)	298(2)	233(2)
2 θ range, deg	3–45	6–105	6–105	7–105	3.5–44
indexing <i>M</i> (20)	na ^a	13.9	29.5	27.6	na
<i>N</i> _{data} (F_o or y_{io})	3389	4951	4951	4901	3673
<i>N</i> _{obs} ($F_o > 2\sigma(F_o)$)	2596	na	na	na	2756
R1, wR2	0.046, 0.115	na	na	na	0.053, 0.119
R_{wp} (Le Bail) ^b	na	0.058	0.053	0.066	na
R_{wp} , R_{wp}^c	na	0.090, 0.124	0.089, 0.126	0.097, 0.126	na
R_{Bragg}^c	na	0.066	0.062	0.067	na
<i>V/Z</i> , Å ³	651	652	716	725	751
stereochemistry C,N	<i>R,R</i> + <i>S,S</i>	<i>R,S</i> + <i>S,R</i>	(mostly) <i>R,R</i> + <i>S,S</i>	4 diastereoisomers	<i>R,R</i> + <i>S,S</i>

^a Not applicable. ^b Weighted profile *R*-factor for powder diffraction analysis after Le Bail refinement. ^c Profile, weighted profile and Bragg *R*-factor for powder diffraction analysis after Rietveld refinement.

fragment, flexible about the acyclic torsion angles (taken from the known single-crystal structure of the α phase), a free chloride ion, and if required, the corresponding additional solvent molecules. Simulated annealing allowed the location and orientation of the used fragments, later refined by the Rietveld method.^{21,22} The quality of the final model can be assessed numerically and graphically by comparing the agreement factors and the residuals of the Le Bail vs Rietveld plots, supplied in the Supporting Information. The Le Bail fitting procedure establishes an upper limit to the quality of fit that could be obtained in a Rietveld refinement calculation for the same experimental powder X-ray diffraction pattern at the same 2 θ range. Thus, the aim of the Rietveld refinement should be to obtain a quality of fit (assessed from the difference profile) as close as possible to that obtained in the profile-fitting calculation.^{23,24} In this case, it was proved that the minor discrepancies still present after full refinement are due not to poor line shape definition but, likely, to “imperfect” definition of the structural model. In the rigid body taken from the single-crystal analysis of the α phase, only torsional angles were freed, together with position and orientation of the molecule(s) within the asymmetric unit. Of course, the definition of the rigid body may not be fully consistent with the “exact” geometry within each polymorph (separately), but this is the fee one must pay to the powder diffraction method when dealing with moderately complex materials, which cannot be treated by the independent atom model commonly adopted in single-crystal diffraction.

According to a very important contribution to the field of structural studies of polymorphic drugs by powder diffraction

methods,²⁵ the relative importance (*impact*) to the χ^2 value of the different geometrical parameters was estimated: position, 250; orientation, 300; torsion, 250; angle, 50; length, 10; chloride counterion, 100. This numerical analysis performed on promazine—an organic molecule of similar complexity than nicardipine hydrochloride—tells that changes in angles and lengths (here fixed) may have a definite impact to the overall agreement factor R_{wp} (mathematically related to χ^2), but to a much lesser extent than the four classes of parameters here refined (position, orientation, torsion and Cl ion location). In order to reach a better match (if any), we have tried to find different minima by the (nonexhaustive) real space approach, running over and over the Monte Carlo procedure, and we have also relaxed some structural constraints. Further improvements in the fit to the diffraction data can indeed be obtained by the introduction of additional parameters to the model: for example, by employing a traditional Rietveld refinement in which the atomic positions are refined individually, or a restrained Rietveld refinement in which atomic positions are refined individually subject to a series of restraints that help to maintain chemical sense. The complexity of our system did not allow the first choice, and, if more freedom (in the less sensitive bond lengths and angles) was added, instability of the refinements was observed also in the second one. After all, the series of restraints suggested in Shankland’s words (ref 13) is nothing else than the definition of a *flexible* rigid body with high restrain weights.

In the structure of the bishydrated and toluene hemisolvate phases, the stereochemistry at the tetracoordinated ammonium

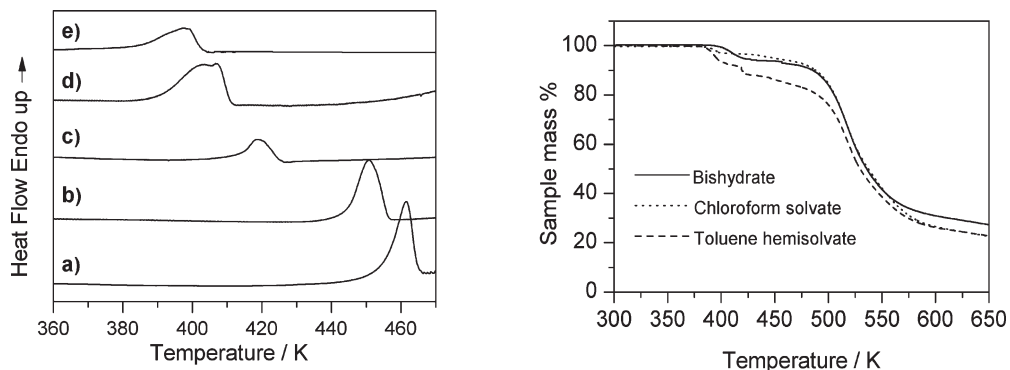


Figure 1. (left) DSC traces of NHc crystalline forms measured at 5 K min^{-1} : (a) α phase, (b) β phase, (c) bishydrate, (d) toluene hemisolvate and (e) chloroform solvate. (right) TG analysis of NHc crystalline solvates measured at 5 K min^{-1} .

residue was checked by adding two methyl residues, instead of a methyl and a proton one, and restraining their site occupancy factors, which eventually refined to 0.74:0.26 and 0.53:0.48, respectively, indicating that these two crystal phases are slightly disordered; the same test was adopted for the stereochemical assignment of the β -NHc phase, but, in this case, the nicardipinium molecules were found ordered, with the *R,S* (and *S,R*) configuration discussed below. The fundamental parameter approach in describing the peak shapes was employed, the background contribution was modeled by a polynomial fit, and preferred orientation effects were described by spherical harmonics approximation (4th order) in the bishydrate NHc phase, and by the March–Dollase model²⁶ (001 pole) in the toluene hemisolvate. A single isotropic thermal parameter was adopted for all atoms and, as such, represents an *unavoidable* simplification of the true thermal motion, normally modeled by approximating dynamic effects by anisotropic displacement parameters. Crystal data and details of the structural analysis, including those for the two phases characterized by single-crystal X-ray diffraction, are reported in Table 1.

X-ray Single-Crystal Analysis. Data collection of the α phase and the chloroform solvate were performed at a temperature of 233 K on a Nonius Kappa CCD equipped with graphite-monochromatized Mo $K\alpha$ radiation ($\lambda = 0.71073 \text{ \AA}$) and a nominal crystal to area detector distance of 36 mm. Intensities were integrated using DENZO and scaled with SCALEPACK. The structures were solved with direct methods SHELXS86²⁷ and refined against F^2 SHELXL97.²⁷ Because of a small size of the plates with thickness between 0.02 and 0.03 mm, both crystals had low diffraction at higher 2Θ values and only reflections until 45° were used for the refinement.

All non-hydrogen atoms were refined with anisotropic displacement parameters, except on disordered minor part of the chloroform molecule. Hydrogen atoms attached to carbon atoms were calculated and refined with isotropic displacement parameters 1.2 or 1.5 times higher than the value of their carbon atoms. Hydrogen atoms at nitrogen atoms were found and refined isotropically. Bond restraints ($d_{\text{NH}} = 0.85 \text{ \AA}$) were used for the chloroform solvate. The chloroform molecule shows a slight position disorder in a ratio of 9:1, whereas the non-hydrogen atoms of the minor part were refined with isotropic displacement parameters.

RESULTS AND DISCUSSION

Thermal Analysis. The DSC analysis obtained for the five crystalline solids of NHc were, in each case, indicative of the occurrence of a new crystal form (Figure 1). The measured

temperatures and melting enthalpies are displayed in Table 2, together with those reported in the literature. TG analysis of the three new discovered crystalline phases are also displayed in Figure 1; the weight losses observed are listed in Table 3.

The total weight losses reported in Table 3 correspond to the elimination of 2 water molecules from the bishydrated phase, 1/2 toluene molecule from the toluene hemisolvate and 1 chloroform molecule from the chloroform solvate, which is consistent with the ratio solvent:NHc molecules observed in the crystal structure analysis. The loss of one chloroform molecule in the TGA occurs in three successive steps, and the loss of 1/2 toluene molecule occurs in two steps. The latter is in agreement with the double peak observed in the DSC analysis. DSC analyses at different heating rates were performed (Figure 2) to confirm the existence of two endothermic peaks for the toluene solvate. These multi-step weight losses are attributed to different interactions between the solvent and the NHc molecules in the crystal structures as discussed in the following sections. Decomposition of NHc is observed by a pronounced weight loss starting at 498 K.

On the basis of the Burger and Rabemberg²⁸ rules and the performed DSC analyses, the α and β forms may be considered as monotonically related since no phase interconversion upon heating is observed. This will be discussed, using the detailed knowledge of the crystal structures, in a following section. Also, according to the temperature of fusion and the heat of fusion rules, the form β should be claimed as metastable, at the absolute zero, with respect to the form α . This hypothesis also matches the experimental observation of the higher solubility (in water) of β -NHc.¹¹

Samples of the chloroform solvate aged for three years at room temperature (protected from light) undergo a solid-state transformation to the thermodynamically stable α form as checked by XRPD (Figure 3). Also, supercritical drying of the chloroform solvate under supercritical CO_2 at a pressure of 13 MPa at 313 K during 8 h induces the transformation into the α polymorph, which is not surprising in view of their similar crystal packing. At variance, the toluene hemisolvate transforms into amorphous NHc on losing the solvent by drying it at 403 K under vacuum (Figure 3, right).

Crystal Structures of α and β Phases. The crystal structure of the α form of NHc was determined from single-crystal data while the crystal structure of the β form of NHc was determined from high quality XRPD data (see above). The cell parameters and other relevant crystallographic data of both crystalline forms of NHc are listed in Table 1. The Rietveld plot for the final fully refined model presented for β -NHc is shown in Figure 4.

Table 2. Temperatures (T in K) and Enthalpies (ΔH in kJ mol^{-1}) of the Melting and Solvent Elimination Processes Experimented by NHc Crystalline Phases on Heating in the DSC at 5 K min^{-1}

	α	β	bishydrate	toluene hemisolvate	chloroform solvate	ref
T/K	457(2)	438(2)	410(1)	387(2)	383(1)	this work
	453.1	440.6				11
	461.2	444.2				2
$\Delta H/\text{kJ mol}^{-1}$	41(4)	39(4)	11(3)	56(5)	27(4)	this work
		43(1)				2

Table 3. Temperatures (T in K) and Weight Loss Percentage (in %) Observed in the TG Analysis of the NHc Solvates on Heating at 5 K min^{-1} ^a

	bishydrate		toluene hemisolvate		chloroform solvate	
	T/K	%	T/K	%	T/K	%
1st wt loss	399	6.5	389	3.1	386	8.7
2nd wt loss			424	4.2	418	2.9
3rd wt loss					424	7.3
total wt loss		6.5		7.3		18.9
decomposition	498		498		499	

^a One water molecule corresponds to a 3.2% weight in a bishydrated solvate. One toluene molecule corresponds to a 16.3% weight in a hemitoluene solvate. One chloroform molecule corresponds to a 18.7% weight in a mono chloroform solvate.

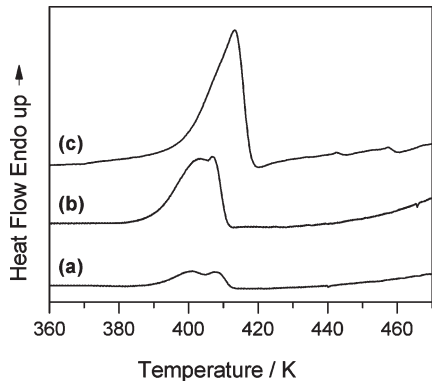


Figure 2. DSC traces of toluene hemisolvate crystalline form measured at (a) 2 K min^{-1} , (b) 5 K min^{-1} and (c) 20 K min^{-1} .

The two unsolvated crystal forms of NHc crystallize into the centrosymmetric $P\bar{1}$ space group with two molecular cations and two (H-bonded) chlorides per unit cell, related by an inversion center, and are racemic salts of intrinsically chiral molecules. The most significant difference between the two phases is the presence, in α -NHc, of enantiomeric molecules of *R,R* and *S,S* configuration at the C and N stereocenters, while only the *R,S* and *S,R* couple is present in the β phase (Figure 5). Strictly speaking, therefore, α -NHc and β -NHc forms contain different molecules, or, more precisely, they are salts of different diastereoisomeric cations. If migration of the “labile” proton on N3 is not occurring, the melts of α -NHc and β -NHc are not equivalent, implying that these two solids are *not* polymorphs of the same chemical species. Not surprisingly, the absence of any interconversion promoted by heating (discussed above) cannot be attributed to the purported monotropic nature of the phase diagram of solid NHc, but, instead, to the high activation energy

required for inversion of the ammonium ion, likely occurring (if occurring at all) only at temperatures higher than the melting point. This said, the term *polymorph* is improperly, but usefully, employed in this paper, with the caveat set above.

As a consequence of this relevant stereochemical property, many conformational parameters show significant differences, particularly when the flexible 2-(benzyl-methyl-amino)ethyl branch is considered (see Table 4), with torsional angles clustering about the 120 and 180° values. Despite these differences, a certain degree of similarity between α -NHc and β -NHc can be devised. As shown in Figure 6, in both phases the NHc molecules give rise to dimers in which two centrosymmetrically related organic cations, and two Cl^- ions, embrace each other generating, through $\text{NH} \cdots \text{Cl} \cdots \text{HN}$ interaction, cyclic moieties, which constitute the repeating unit of the whole crystals. Worthy of note, in both cases these supramolecular synthons show chloride ions simultaneously interacting with the chiral ammonium residue of one molecule and the NH portion of 1,4-dihydropyridine ring of the other one.

Crystal Structures of the Hydrate, the Chloroform and the Toluene Hemisolvate. Three new crystalline phases of NHc were prepared using the standard crystallization methods described in Materials and Methods. In addition, the chloroform solvate was also prepared in the form of a crystalline powder from GAS and DELOS methodologies.^{12,14–18} These two environmentally friendly techniques use compressed CO_2 either as antisolvent (GAS method) or as cosolvent (DELOS method) for the production of nano or micro particulated solids with controlled structural parameters, such as morphology, size and narrow size distribution.^{29–31}

Suitable single crystals for structure determination from single-crystal X-ray diffraction of the chloroform solvate were successfully prepared, while, in the other two cases, the crystal structure was determined from XRPD data since all the attempts to prepare single crystals of enough quality for single-crystal X-ray diffraction were not successful.¹⁹ The cell parameters and other relevant crystallographic data of the three new solvated phases of NHc are listed in Table 1. The Rietveld plots for the final fully refined models are shown in Figure 7.

The chloroform solvate form of NHc crystallizes in the triclinic $P\bar{1}$ space group and contains two enantiomeric protonated nocardipine molecules, two chloride ions and two CHCl_3 molecules. The stereochemical description of the organic moieties is *R,R* (and *S,S*), and, as expected, the chloride ions interact with the protonated amine and the heterocyclic NH moiety, giving rise to cyclic dimers similar, but not equal, to those found in the α form. The most striking difference, as shown in Figure 8, is the presence of two ancillary $\text{Cl} \cdots \text{HC}$ contacts with the chloroform molecules, making the chloride ions tris, and not only bis, “coordinated”. The solvent molecules show a 90:10 disorder of the rotational type, maintaining the CHCl_3 moiety hinged about the $\text{CH} \cdots \text{Cl}$ vector.

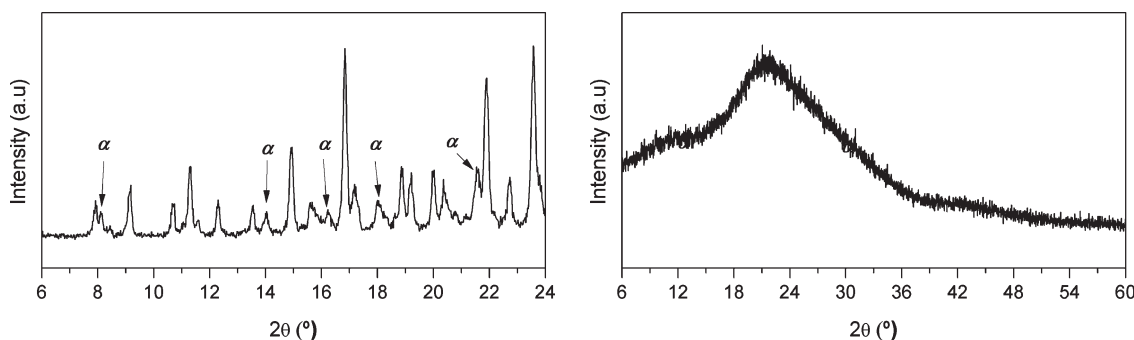


Figure 3. (left) XRPD pattern of an aged sample—three years at room temperature—of the chloroform solvate showing the mixture of α -NHc and the chloroform solvate. The reflections used to identify the α polymorph are marked with an arrow. (right) XRPD pattern of a sample of the toluene hemisolvate measured after drying at 403 K under vacuum.

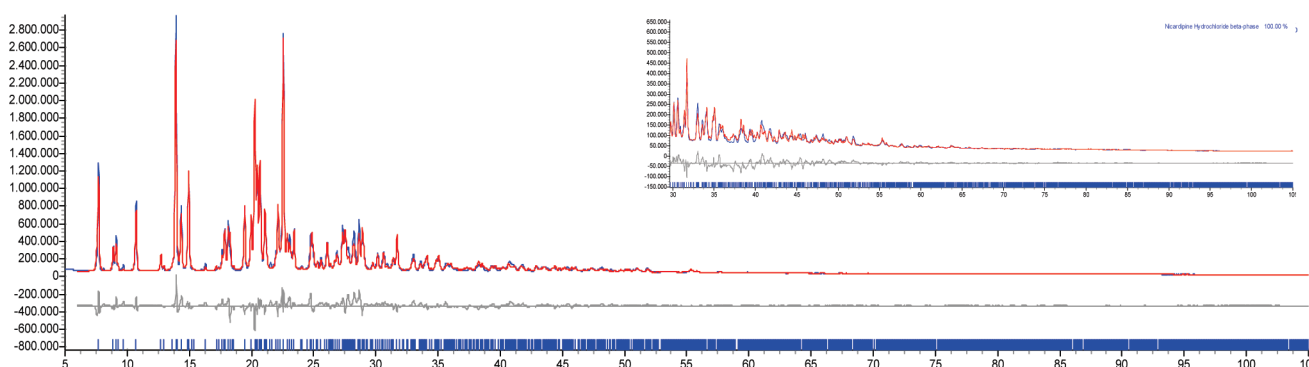


Figure 4. Rietveld refinement plot for β -NHc. The difference plot and peak markers are represented at the bottom. The inset shows the high angle portion at a magnified scale ($5\times$).

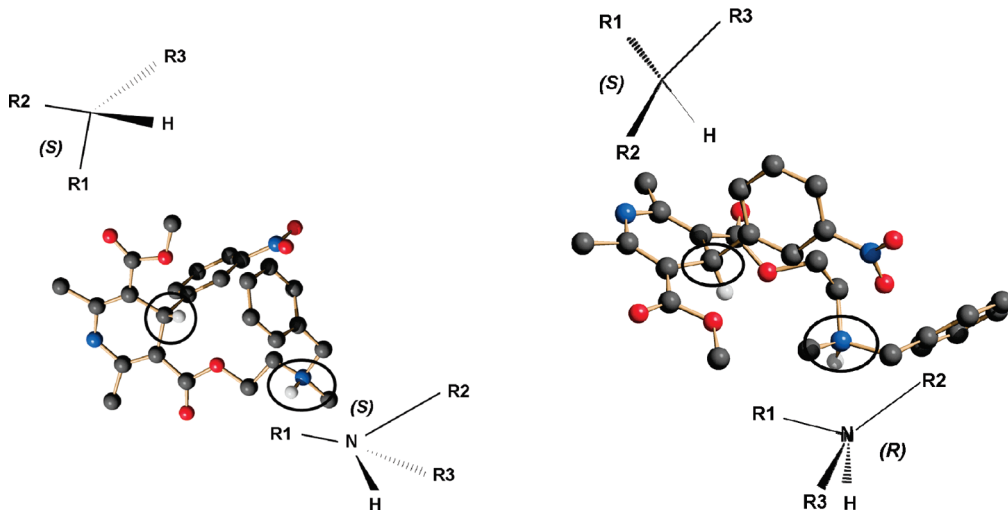


Figure 5. Representation of a molecule of NHc in α -NHc (left) and β -NHc (right) showing the configuration of the two stereocenters. The unit cell of each polymorph contains the represented molecule and its enantiomer, which is generated by symmetry. Only the hydrogen atoms united to the asymmetric carbon and nitrogen are represented. R1, R2, and R3 represent the priorities attributed to each substituent according to the Cahn–Ingold–Prelog rules followed to assign R or S configuration.

Due to the identity of stereoisomers in this solvated phase and in the α -NHc phase and thanks to their similar molecular arrangement (and despite a non-easily recognizable similarity of the crystal packing), it is not surprising that the α form is recovered from the chloroform solvate after spontaneous solvent loss upon aging for three years or after CHCl_3 extraction via supercritical drying.

The remaining phases, *i.e.* the toluene hemisolvate and the bishydrated form of NHc, are isomorphous compounds, crystallizing in the centrosymmetric $P2_1/c$ space group. Each unit cell contains four molecules of NHc and eight water or two toluene molecules, respectively. The crystal packing of the toluene hemisolvate and the bishydrate forms is depicted in Figure 9, with toluene molecules, located on inversion centers, showing a

Table 4. Relevant Structural Data of Crystal Forms α - and β -NHC^a

phase	distance [Å]		torsion angles [deg]			
	Cl \cdots N3 ^b	Cl \cdots N1 ^b	C5—C1—C6—C7 ^b	C2—C12—O4—C13 ^b	C12—O4—C13—C14 ^b	O2—N2—C8—C9 ^b
α	3.03	3.18	111.7(2)	174.2(2)	-174.0(2)	179.1(2)
β	2.88	3.49	118.8(2)	-122.2(2)	-118.3(1)	23.7(8)

^a Esd's in parentheses. ^b Refer to Scheme 1 for the numbering assignment.

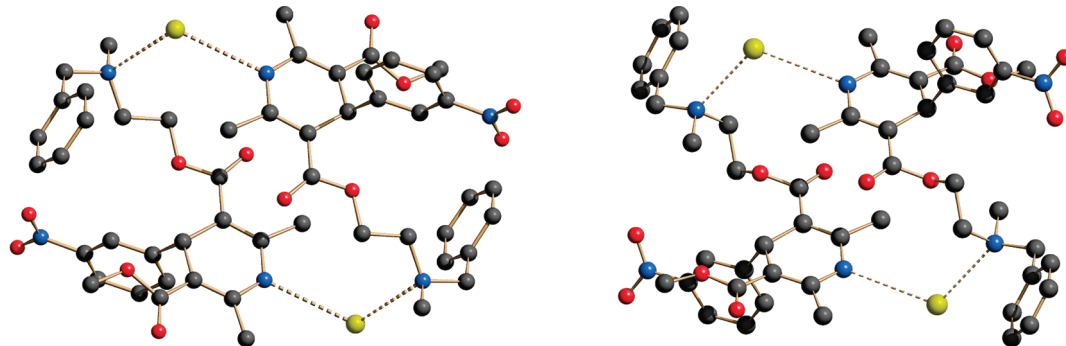


Figure 6. Centrosymmetric synthons (discussed in the text) for α -NHC (left) and β -NHC (right), similarly oriented, in order to highlight the structural similarities.

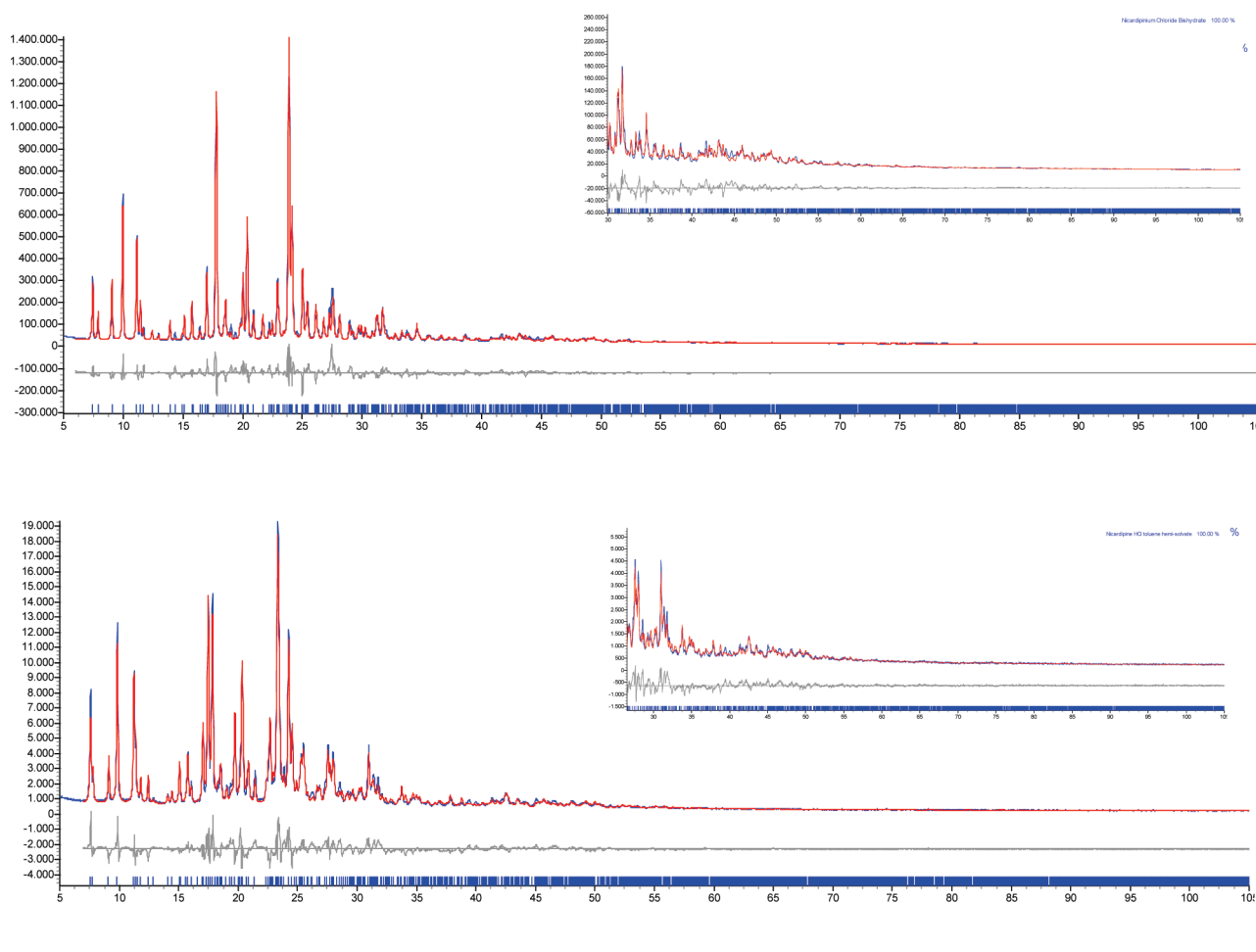


Figure 7. Rietveld refinement plots for the bishydrated phase of NHc (top) and the toluene hemisolvate phase (bottom) with difference plot and peak markers at the bottom. The inset shows the high angle portion at a magnified scale (5 \times).

crystallographically imposed 50:50 disorder. In these crystals, the stereochemistry is, again, *R,R* and *S,S*, although a minor component of the *R,S* and *S,R* configurations is present (with the necessary caveat set by the quality of structural results from XRPD data alone, which do not allow the definition of high

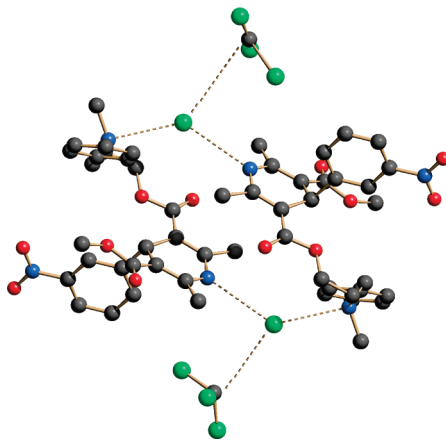


Figure 8. Schematic drawing of the centrosymmetric molecular dimer present in the chloroformate form of NHc, with the solvent molecules hydrogen-bonded to the chloride anions. Only the major components of the disordered CHCl_3 molecules are shown here.

quality models as in conventional single-crystal analyses). This molecular disorder can be easily understood if the location of the chloride anions is addressed: these ions are deeply buried within an *all-H* cavity, with only one $\text{NH} \cdots \text{Cl}$ interaction (that with the heterocyclic N atom). Indeed, the configuration of the protonated nitrogen atom of the ammonium residue, in both crystal structures, is not fixed by any evident hydrogen bond to the Cl^- ions, thus allowing the formation of a solid solution of two different diastereoisomeric pairs, occupying the same crystallographic sites, although with different populations.³²

The remaining fragments, like the water molecules of the bishydrated form of NHc, are hosted in lattice cavities, clustering in tetrameric moieties about inversion centers, and only weakly interacting with the remaining portions of the crystal. Similarly, toluene molecules fall in identical cavities, as shown in Figure 9.

In the three solvated phases of NHc discussed in this paper, the solvent molecules are accommodated in the space generated between layers of adjacent NHc molecules packed with the centrosymmetrically related nitrobenzene groups, pointing in opposite directions (see Figure 10).

The toluene molecule in the crystal structure of the toluene hemisolvate is located between two nitrobenzene groups of adjacent layers separated by 7.4 Å. These aromatic rings are stacked in a nearly parallel manner and, therefore, stabilize the crystal by the presence of $\pi-\pi$ interactions of the graphitic type. We have experimentally observed that removal of the toluene

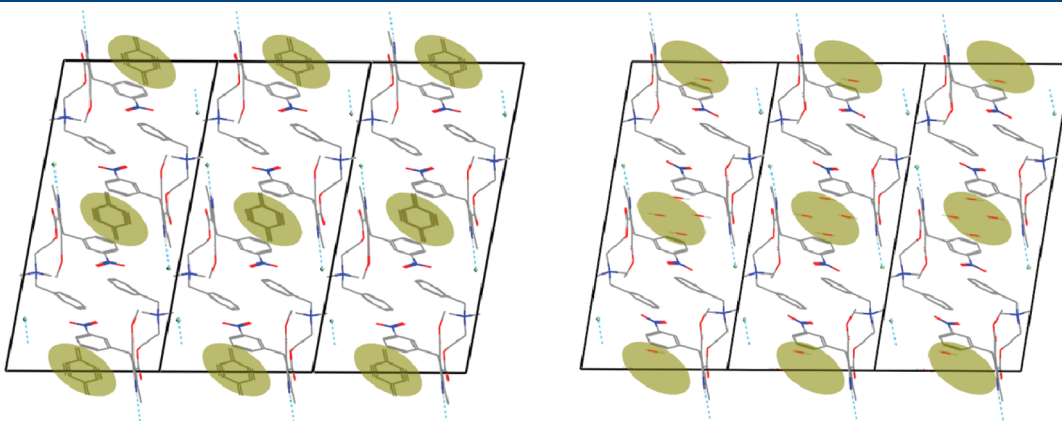


Figure 9. Crystal packing of the toluene (left) and the bishydrate (right) phases of NHc projected in the (a,c) plane. The cavity hosting the solvent is highlighted in gray. Hydrogen atoms not involved in hydrogen bonds or water molecules are omitted for clarity.

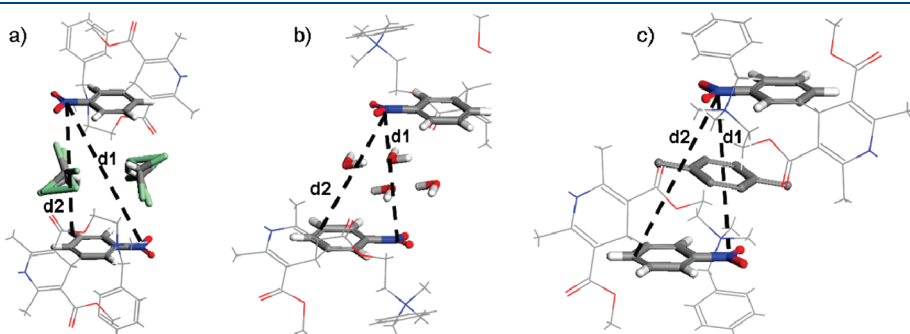


Figure 10. Scheme showing the packing relation between the solvent and the nitrobenzene fragment of the NHc molecule in the crystal structure of (a) the chloroform solvate, (b) the bishydrate and (c) the toluene hemisolvate. Note that the methyl group of the toluene molecule in the toluene solvate occupies the two positions with a 50% probability due to the disorder imposed by symmetry. The solvent molecules and the nitrobenzene fragment are highlighted for clarity. The cavities hosting the solvent molecules can be defined by the length of the $\text{N}2-\text{N}2'$ ($d1$) and $\text{N}2-\text{C}11'$ ($d2$) vectors; $d1$ and $d2$ values (left to right) 9.97 and 8.85 Å; 7.85 and 8.37 Å; 7.48 and 8.27 Å.

Table 5. Relevant Molecular Structural Data of the Three NHc Solvates^a

phase	distance [Å]		torsion angle [deg]		
	Cl···N3 ^b	Cl···N1 ^b	C5—C1—C6—C7 ^b	C2—C12—O4—C13 ^b	C12—O4—C13—C14 ^b
chloroform solvate	3.13	3.30	105.2(4)	175.3(3)	−166.0(3)
bishydrate	(4.33)	3.26	156.7(3)	168(1)	−125(1)
toluene hemisolvate	(4.27)	3.23	160.5(3)	169(1)	−112(1)

^a Esd's in parentheses. ^b Refer to Scheme 1 for the numbering assignment.

molecules by moderate heating generates an amorphous phase; on the contrary, the chloroform phase can eliminate the guest molecules and regenerate the thermodynamically stable α phase. Moreover, the larger space available between the different nicardipinium ions in the crystals of the chloroform phase can also easily accommodate (two) water molecules. Accordingly it is not surprising that the bishydrated phase can be quantitatively recovered upon exposing the chloroform solvate to humidity in the presence of diethyl ether which has high miscibility with chloroform. As presented above for the unsolvated species, the relevant structural parameters of the three new solvates of NHc are listed in Table 5.

CONCLUSIONS

In this study three new solvated forms of NHc, namely, a bishydrate, a toluene hemisolvated and a chloroform solvate phase, have been isolated. The crystal structures of these newly discovered solvates and those of the already known α and β phases of NHc have been determined. Conventional structural analysis by single-crystal X-ray diffraction methods was possible only for the α -NHc polymorph and the chloroform solvate, demonstrating that, in these two crystal phases, racemates of the *R,R* and *S,S* diastereoisomers are present. For the three remaining crystal phases (β -NHc, the bishydrate and the toluene hemisolvate phases), in the absence of suitable specimens of decent quality and size, we resorted to XRPD analysis; using direct-space Monte Carlo simulated annealing methods and (semiflexible) rigid body description of the large organic fragment, their crystal structures were solved, and eventually refined, by the Rietveld whole pattern modeling technique. The derived structures allowed the interpretation of the stereochemical preferences in the different phases, such as the existence of different racemates, or of different diastereoisomers within the same crystal phase.

The results presented here have largely benefited from the recent development of powder X-ray diffraction methodologies to determine crystal structures of molecular compounds with a high degree of complexity (in terms of high molecular flexibility and unit cell content) even from well-conditioned, and easily accessible, laboratory data; it goes without telling, the quality of the structural models that a structure determination from powder X-ray diffraction can provide is much lower than that obtainable from single-crystal X-ray diffraction experiments. Nevertheless, if the accurate evaluation of intramolecular geometrical parameters (bond distances and angles) is neglected, knowledge on crystal packing and intermolecular interactions can be easily accumulated. After all, while the connectivity pattern and the overall (flexible) geometry could be taken from the fortuitous occurrence of single-crystal structures of NHc polymorphs, the determination of the relative stereochemistry of the different stereogenic centers and of the most relevant packing interactions (including hydrogen bonds and interionic interactions) could be well characterized, allowing a sensible interpretation of the rich (pseudo)polymorphism of NHc. With the example of the

(pseudo)polymorphs of nicardipine it is shown how powder X-ray diffraction is a powerful technique to determine the crystal structure, including the stereochemistry, of highly flexible drugs or drug delivery systems that are difficult or even impossible to crystallize in a reasonable time scale as suitable single crystals in terms of size and quality for single-crystal X-ray structure determination.

Galenic characterization of these new crystalline phases is now of utmost importance in order to evaluate its potential use as a drug. Further work is in due course to evaluate the availability of NHc bishydrate in new formulations.

CIF files are available at CCDC deposition numbers 785472, 785473, 785474, 785475, and 785476.

ASSOCIATED CONTENT

S Supporting Information. Comparison of the structureless (Le Bail) and final Rietveld refinement plots. This material is available free of charge via the Internet at <http://pubs.acs.org>.

AUTHOR INFORMATION

Corresponding Author

*N.V.: CONSEJO SUPERIOR DE INVESTIGACIONES CIENTÍFICAS, Institut de Ciència de Materials de Barcelona (CSIC), Campus de la Universidad Autónoma de Barcelona, E-08193 Bellaterra; e-mail, ventosa@icmab.es; tel, +34-93-580 18 53; fax, 34-93-580 57 29. N.M.: Università degli Studi dell'Insubria, Dipartimento di Scienze Chimiche e Ambientali Via Valleggio, 11 22100 Como, Italy; e-mail, Norberto.Masciocchi@uninsubria.it; tel, +39-031-2386627; fax, +39-031-2386119.

ACKNOWLEDGMENT

We thank one referee for stimulating a better presentation of the paper. This work was supported by DGI Spain under projects EMOCIONA (CTQ2006-06333/BQU) and POMAS (CTQ-2010-19501). We acknowledge financial support from Instituto de Salud Carlos III, through "Acciones CIBER". The Networking Research Center on Bioengineering, Biomaterials and Nanomedicine (CIBER-BBN) is an initiative funded by the VI National R&D&I Plan 2008-2011, Iniciativa Ingenio 2010, Consolider Program, CIBER Actions and financed by the Instituto de Salud Carlos III with assistance from the European Regional Development Fund. The authors thank Jordi Balaguer for his assistance in thermal measurements. M.M. thanks the Spanish Council of Scientific Research (CSIC) for her doctoral grant (I3P-BPD2002). N.V. thanks Banco de Santander for the chair of Knowledge and Technology Transfer Parc de Recerca UAB-Santander. We also thank TECNIO network for financial support on technological transfer activities related to this work.

■ REFERENCES

- (1) Muñoz Alameda, L. E.; Barcina Sánchez, M. Intravenous nicardipine: a new calcium antagonist for perioperative use. *Rev. Esp. Anestesiol. Reanim.* **2001**, *48* (2), 71–80.
- (2) (a) Teraoka, R.; Otsuka, M.; Matsuda, Y. Evaluation of photostability of solid-state nicardipine hydrochloride polymorphs by using Fourier-transformed reflection–absorption infrared spectroscopy—effect of grinding on the photostability of crystal form. *Int. J. Pharm.* **2004**, *286*, 1–8. (b) Kohinata, T.; Fuji, M.; Nakamura, S.; Hamada, N.; Yonemochi, E.; Katsuhide, T. Quantitative determination of amorphous nicardipine hydrochloride in long acting formula (NIC-LA) using light anhydrous silicic acid. *Chem. Pharm. Bull.* **2004**, *52* (12), 1451–1457.
- (3) Higuchi, S.; Shiobara, Y. Pharmacokinetic studies on nicardipine hydrochloride, a new vasodilator, after repeated administration to rats, dogs and humans. *Xenobiotica* **1980**, *10*, 447–454.
- (4) Graham, D. J. M.; Dow, R. J.; Hall, D. J.; Alexander, O. F.; Mroszczak, E. J.; Freedman, D. The metabolism and pharmacokinetics of nicardipine hydrochloride in man. *Br. J. Clin. Pharmacol.* **1985**, *20*, 23S–28S.
- (5) Varon, J.; Marik, P. E. The diagnosis and management of hypertensive crises. *Chest* **2000**, *118*, 214–227.
- (6) Sorin, E. M.; Clissold, S. P. Nicardipine. A review of its pharmacodynamic and pharmacokinetic properties, and therapeutic efficacy, in the treatment of angina pectoris, hypertension and related cardiovascular disorders. *Drugs* **1987**, *33* (4), 296–345.
- (7) (a) <http://www.rxlist.com/cardene-iv-drug.htm>. (b) <http://www.drugs.com/pro/cardene.html>.
- (8) Bernstein, J. *Polymorphism in Molecular Crystals*, 1st ed.; Clarendon Press: Oxford, 2002; pp 9–19.
- (9) McCrone, W. C. In *Physics and Chemistry of the Organic Solid State*, 1st ed.; Fox, D.; Labes, M. M., Weissberger, A., Eds.; Interscience Publishers: London, 1965; Vol. 2, pp 725–767.
- (10) Iwanami, M.; Shibanuma, T.; Fujimoto, M.; Kawai, R.; Tamazawa, K.; Takenaka, T.; Takahashi, K.; Murakami, M. Synthesis of Water-soluble Dihydropyridine Vasodilators. *Chem. Pharm. Bull.* **1979**, *27*, 1426–1433.
- (11) Yan, J.; Giunchedi, P. Characterization of α and β crystalline forms of nicardipine hydrochloride. *Boll. Chim. Farm.* **1990**, *129*, 276–278.
- (12) Muntó, M.; Moreno, E.; Sala, S.; Ventosa, N.; Veciana, J. Tuning of Nicardipine hydrochloride polymorphic nature and purity controlled by CO_2 based processes crystallization parameters. Unpublished results.
- (13) Kauffman, G. B.; Myers, R. Pasteur's resolution of racemic acid: A sesquicentennial retrospect and a new translation. *Chem. Educ.* **1998**, *3* (6), 1–18.
- (14) Ventosa, N.; Sala, S.; Torres, J.; Llibre, J.; Veciana, J. Depressurization of an Expanded Liquid Organic Solution (DELOS): A New Procedure for Obtaining Submicron- or Micron-Sized Crystalline Particles. *Cryst. Growth Des.* **2001**, *1*, 299–303.
- (15) Gimeno, M.; Ventosa, N.; Sala, S.; Veciana, J. Use of 1,1,1,2-Tetrafluoroethane (R-134a)-Expanded Liquids as Solvent Media for Ecoefficient Particle Design with the DELOS Crystallization Process. *Cryst. Growth Des.* **2006**, *6* (1), 23–25.
- (16) Ventosa, N.; Sala, S.; Veciana, J. DELOS process: a crystallization technique using compressed fluids: 1. Comparison to the GAS crystallization method. *J. Supercrit. Fluids* **2003**, *26*, 33–45.
- (17) (a) Ventosa, N.; et al. Method for precipitating finely divided solid particles. Patent number: WO 0216003. (b) Ventosa, N.; Veciana, J.; Sala, S.; Cano, M.; Method for obtaining micro- and nano-disperse systems. ESP P200500172, International number WO2006/0799889, 2005.
- (18) Ventosa, N.; Veciana, J.; Sala, S.; Muntó, M.; Cano, M.; Gimeno, M. New technologies for the preparation of micro- and nanostructured materials with potential applications in drug delivery and clinical diagnostics. *Contrib. Sci.* **2005**, *3* (1), 11–18.
- (19) David, W. I. F.; Shankland, K. *Structure determination from powder diffraction data*, 1st ed.; McCusker, M., Baerlocher, Ch., Eds.; Oxford University Press: Oxford, 2002.
- (20) Bruker AXS. *TOPAS-R V 3.0 The new dimension in profile and structure analysis*; Karlsruhe, Germany, 2005.
- (21) Young, R. A. *The Rietveld Method*; Oxford University Press: Oxford, 1995.
- (22) McCusker, L. B.; Von Dreele, R. B.; Cox, D. E.; Louë, D.; Scardi, P. Rietveld refinement guidelines. *J. Appl. Crystallogr.* **1999**, *32*, 36–50.
- (23) Harris, K. D. M. Aspects on validation in the structure determination of organic materials from powder x-ray diffraction data. *Z. Kristallogr.* **2007**, *S26*, 45–51.
- (24) Pan, Z.; Cheung, E. Y.; Harris, K. D. M.; Constable, E. C.; Housecroft, C. E. A Case Study in Direct-Space Structure Determination from Powder X-ray Diffraction Data: Finding the Hydrate Structure of an Organic Molecule with Significant conformational Flexibility. *Cryst. Growth Des.* **2005**, *5*, 2084–2090.
- (25) Shankland, K. Global Rietveld Refinement. *J. Res. Natl. Inst. Stand. Technol.* **2004**, *109*, 143–154.
- (26) (a) March, A. Mathematische Theorie der Regelung nach der Korngestalt bei affiner Deformation. *Z. Kristallogr.* **1932**, *81*, 285–297. (b) Dollase, W. A. Correction of intensities for preferred orientation in powder diffractometry: Application of the March model. *J. Appl. Crystallogr.* **1986**, *19*, 267–272.
- (27) (a) Sheldrick, G. M. *SHELXS86, Program for the Solution of Crystal Structures*; University of Göttingen: Germany, 1986. (b) Sheldrick, G. M. *SHELXL97, Program for Crystal Structure Refinement*; University of Göttingen: Göttingen, Germany, 1997. (c) Sheldrick, G. M. A short history of SHELX. *Acta Crystallogr.* **2008**, *A64*, 112–122.
- (28) Burger, A.; Ramberger, R. On the polymorphism of pharmaceuticals and other molecular crystals. I. *Mikrochim. Acta* **1979**, *II*, 259–271.
- (29) Sala, S.; Elizondo, E.; Moreno, E.; Calvet, T.; Cuevas-Diarte, M. A.; Ventosa, N.; Veciana, J. Kinetically driven crystallization of a pure polymorphic phase of stearic acid from CO_2 -Expanded Solutions. *Cryst. Growth Des.* **2010**, *10* (3), 1226–1232.
- (30) Muntó, M.; Ventosa, N.; Sala, S.; Veciana, J. Solubility behaviours of ibuprofen and naproxen drugs in liquid “ CO_2 -organic solvent” mixtures. *J. Supercrit. Fluids* **2008**, *47*, 147–153.
- (31) Muntó, M.; Ventosa, N.; Veciana, J. Synergistic solubility behaviour of a polyoxyalkylene block co-polymer and its precipitation from liquid CO_2 -expanded ethanol as solid microparticles. *J. Supercrit. Fluids* **2008**, *47*, 290–295.
- (32) Srivastava, S.; Ter Horst, J. H. Racemic compounds, Conglomerate, or Solid Solution: Phase Diagram Screening of Chiral Compounds. *Cryst. Growth Des.* **2010**, *10* (4), 1808–1812.